Biochimica et Biophysica Acta, 1029 (1990) 24–32
Elsevier

BBAMEM 75030

Spectroscopic and physicochemical studies on the interactions of reversible H^+/K^+-ATPase inhibitors with phospholipid bilayers

David G. Reid, Lesley K. MacLachlan, Robert C. Mitchell, Michael J. Graham, Michael J. Raw and Paul A. Smith

Physical Organic Chemistry Department, Smith Kline & French Research, Welwyn (U.K.)

(Received 10 May 1990)

Key words: Phospholipid bilayer; DSC; ATPase, H^+/K^+-; ATPase inhibitor; Fourier transform

Three complementary techniques, differential scanning calorimetry (DSC), Fourier transform infrared (FT-IR) spectroscopy and nuclear magnetic resonance (NMR) spectroscopy, have been used to characterise the interactions between dimyristoylphosphatidylcholine (DMPC) model biological membranes and two non-covalent inhibitors of the gastric (H^+, K^+)-ATPase. DSC, FT-IR and deuterium NMR studies of side-chain perdeuterated DMPC (DMPC-d_{54}) support the prediction, based on physical property measurements, that SK&F 96079 partitions readily into phospholipid bilayers, resulting in a slight but measurable disordering of the lipid hydrocarbon side-chain motion and a concomitant reduction in the co-operativity and onset temperature of the gel to liquid crystalline phase transition. However, FT-IR and deuterium NMR studies show that the bilayer structure remains intact even at high (1:4) compound to lipid molar ratios. Proton (^1H) NMR nuclear Overhauser effect determinations in sonicated codispersions reveal details of the membrane bound conformations of SK&F 96079. The structurally related analogue SK&F 96464, also studied by ^1H-NMR, can be shown, by interpreting the effects of nitroxide-labelled fatty acid relaxation probes, to adopt a well-defined orientation relative to the bilayer, in contrast to SK&F 96079. This orientation directs the proton at the 5-position of the quinoline ring towards the hydrophobic centre of the bilayer, and the quinoline 8-methoxy group towards the surface and hence the aqueous phase. Molecular modelling has been used to rationalise this orientation in terms of hydrogen bonds between the amino NH group of SK&F 96464 and the *sn*-1 carbonyl group of DMPC, and between the NH group of the protonated quinoline ring of SK&F 96464 and the DMPC phosphodiester group.

Introduction

The gastric (H^+, K^+)-ATPase is a large membrane spanning protein which uses the energy generated by the hydrolysis of ATP to pump hydrogen ions into the mammalian stomach against an enormous activity gradient in exchange for potassium, and thus maintain its extremely low pH value [1–4]. Recently, the discovery of inhibitors of this enzyme has promised pharmalogically novel methods of controlling ulcers by moderating gastric acidity. These compounds may challenge the very successful histamine H_2-receptor antagonists [5], which block gastric acid secretion by indirect inhibition of hormonal stimulation [6].

SK&F 96079 (I) and SK&F 96464 (II) are non-covalent inhibitors of the (H^+, K^+)-ATPase; their mode of action appears analogous to that of other compounds reported to be competitive with K^+ [7–9]. The compounds apparently bind in their protonated, cationic state to the luminal, stomach facing, side of the ATPase, possibly although not necessarily at the primary K^+ binding site [9].

The interactions of drugs which act on membrane-bound receptors, and membranes themselves, have been the subject of much experiment and speculation. The importance of membrane interactions to the efficacy of drugs such as local or general anaesthetics is well accepted. Its significance in the action of other drugs such as, for instance, the β-adrenergic antagonists, has been suggested [10], and the hypothesis has been proposed that increasing the bulk of hydrophobic regions of a compound can increase its affinity for the target receptor by 'anchoring' it in the membrane and facilitating the interaction of the pharmacophore with the active site [11]. Irrespective of whether an interaction

Abbreviations: DSC, differential scanning calorimetry; NMR, nuclear magnetic resonance; DMPC, dimyristoyl phosphatidylcholine

Correspondence: D.G. Reid, Smith Kline & French Research Ltd., The Frythe, Welwyn, Herts. AL6 9AE, U.K.

with a membrane is essential or advantageous to a medicinal compound's mode of action, it can have a profound influence on factors such as gastrointestinal absorption, biodistribution, access to intracellular environments, and penetration of the blood-brain barrier.

SK&F 96079 has very high octanol-water and cyclohexane-water partition coefficients (log $P_{oct} = 4.32$, log $P_{cyh} = 2.58$) (Mitchell, R.C., unpublished results), which suggests that its interactions with biological membranes may influence its pharmacodynamic and pharmacokinetic properties. This paper reports DSC, FT-IR and deuterium NMR studies of the effects of I on the properties of a model membrane, and proton NMR, including NOE and spin probe, investigations of the membrane location, conformation and orientation of this compound and the structurally closely related II. These data have enabled us to construct a model of the mechanism of interaction of the latter with an individual membrane constituent phospholipid.

Materials and Methods

Sample preparation

All FT-IR, DSC and deuterium NMR determinations were performed on liposomal dispersions in the presence of excess water. A weighed quantity (ca. 15 mg) of DMPC-d_{54} (Cambridge Isotope Laboratories, Woburn, MA) was dissolved in a small (ca. 100 μl) volume of chloroform and, where appropriate, a known quantity of compound was added in the same solvent. The pure lipid solution or compound/lipid mixture was evaporated under a gentle stream of nitrogen gas and finally pumped to complete dryness under vacuum overnight. The resultant film was then dispersed in 0.5 ml of deuterium-depleted water (Sigma) by alternately vortex stirring and warming for a few minutes. After deuterium NMR experiments had been performed, appropriate aliquots of the dispersion were freeze-dried, resuspended in D_2O (99.98 atom % D, Aldrich) and used in FT-IR and DSC studies. The final pH values of the dispersions were determined with a 3 mm glass electrode and found to lie between 7 and 8.

Proton NMR studies were performed on sonicated dispersions. Compound-lipid films, or films containing small mole fractions of the fatty acid spin probes, 5- or 16-doxyl stearic acid (Aldrich), were prepared as described above. The films were then dispersed in 0.5 ml D_2O and sonicated by means of a Gallenkamp Soniprep 150 equipped with a microtip probe.

At the end of each series of experiments, DMPC was checked for purity by thin layer chromatography in chloroform/ methanol/ ammonia; phospholipid degradation was found to be negligible.

FT-IR

The lipid dispersion was placed in a Specac 20500 heatable infrared cell fitted with CaF_2 windows and a 50 μm Teflon spacer. The cell was held in a water-jacketted holder supplied with water from a Neslab EX100DD circulating water bath and a Neslab FTC-350A flow through cooler, controlled by a Neslab MTP-5 programmer. The stability of the temperature at the cell window, measured via a thermocouple, was better than ± 0.1°C. Spectra were recorded on a Perkin-Elmer 1750 Fourier transform infrared spectrometer, equipped with an interleave accessory and a TGS detector, over the temperature range 9–35°C at 1° intervals. For each spectrum, 25 scans were averaged, at a resolution of 4 cm^{-1}, using a medium Norton-Beer function for apodization. The sample compartment was continuously purged with dry nitrogen during the course of an experiment. The peak position of the band at ca. 2090 cm^{-1}, arising from the symmetric stretching vibrations of the CD_2 groups in the lipid acyl chains [12], was determined from the second derivative of the 'single beam' spectrum i.e., before subtraction of the spectrum of D_2O; the second derivative was generated using the Perkin-Elmer routine DERIV with a width of 13 points. The collection, storage and manipulation of the spectral data was fully automated by linking OBEY programs

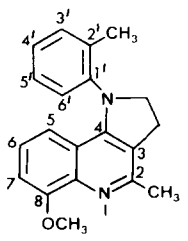

SK&F 96079

I

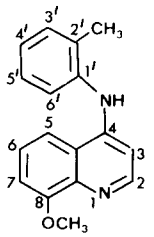

SK&F 96464

II

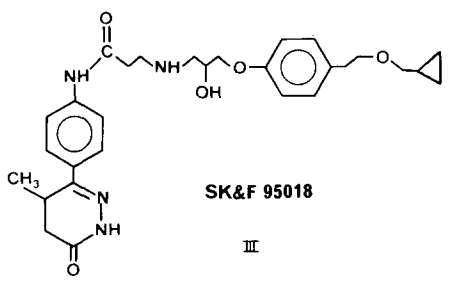

SK&F 95018

III

on the Perkin-Elmer 7000 data station to the temperature program on the Neslab MTP-5 programmer.

DSC

Thermograms were obtained on a Perkin-Elmer DSC-2C fitted with a dry-box and sub-ambient accessories. The dry-box was purged with dry nitrogen and the DSC head cooled down to 0 °C using a Perkin-Elmer Intracooler I. This was done during the night before the experiments were carried out in order to ensure a stable baseline.

Ca. 4 mg of lipid dispersion were weighed into an aluminium volatile sample pan. A lid was placed on top and the pan was sealed using a Perkin-Elmer volatile sample pan sealer. The pan was then placed in the dry-box and from there transferred to the sample side of the DSC head. An empty sealed volatile sample pan was placed in the reference side.

The samples were scanned between 0 ° and 60 °C at a heating rate of 10 °C/min. In order to ensure good contact between the dispersion and the bottom of the sample pan, the samples were taken through a heating run and then cooled at 40 °C/min prior to any data being recorded. Cooling and rescanning of the samples showed that the transitions were reversible.

Thermograms were stored on a Perkin-Elmer 3600 Data Station and were normalised and rescaled (0.08 mcal/s, 10 °–40 °C) before being plotted on a Perkin-Elmer TADS-1 plotter.

NMR

All NMR spectra were acquired on a Bruker AM360, in the Fourier transform mode using quadrature acquisition characteristics. Deuterium NMR was performed at 55MHz in a Bruker VSP 5mm probe without using a field-frequency lock. $\pi/2$ pulses of between 12 and 13 μs were used with a sweep width of 50 kHz and interpulse delay of 100 ms. Lack of a high power transmitter and fast digitiser precluded use of a quadrupolar echo sequence. As a consequence, line shapes were somewhat distorted away from the expected idealised Pake lineshape. We do not believe that this precludes accurate measurements of quadrupolar splittings. Depending on linewidth, and signal to noise requirements, between 10000 and 100000 scans were acquired. Proton NMR was performed on a dedicated ^{1}H 5-mm probehead. Standard presaturation or DANTE solvent suppression techniques [13] were employed to minimise the signal from residual solvent protons.

Results

FT-IR and DSC

Fig. 1a shows a plot of the wavenumber maximum of the band at ca. 2090 cm^{-1} due to the symmetric stretching vibrations of the CD_2 groups in the lipid acyl chains, $\nu_s(CD_2)$, versus temperature for DMPC-d_{54} dispersed in D_2O. Below 20°C, $\nu_s(CD_2) \simeq 2090$ cm^{-1} which indicates that the hydrocarbon side-chains are in a gel state and contain a high proportion of trans conformers. Between 20 and 24°C, $\nu_s(CD_2)$ increases sharply due to the transition from the gel to the liquid crystal state, and the concomitant increase in the proportion of gauche conformers [12].

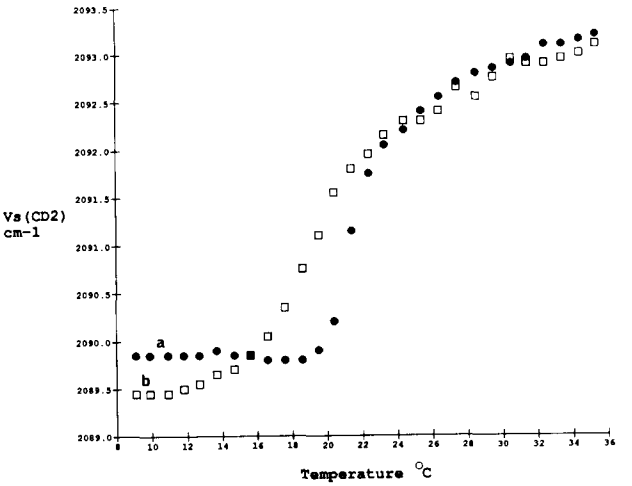

Fig. 1. Plots of $\nu_s(CD_2)$ versus temperature of (a) pure DMPC-d_{54} in excess D_2O, (b) in the presence of 0.125 mol equivalents of I.

The effects of incorporating I into DMPC-d_{54}/D_2O dispersions on the $\nu_s(CD_2)$/temperature profile were examined at compound/lipid molar ratios of 1 : 20, 1 : 8 and 1 : 4. I has little effect at a 1 : 20 ratio; however at a 1 : 8 ratio (Fig. 1b) incorporation of the compound results in a broadening of the transition, and reduction of its onset by 4 to 5°C. Above and below the transition, I has no significant effect on $\nu_s(CD_2)$. Very similar effects on the temperature and shape of the transition are revealed by the DSC results (not shown).

Deuterium NMR

The effects of increasing molar ratios of I on the deuterium NMR characteristics of DMPC-d_{54} dispersed in water at 28°C are summarised in Table I, which shows quadrupolar splitting values ($\Delta\nu_Q$) and derived segmental order parameters (S_{CD}). An increasing mole fraction of the compound produces a small but consistent (ca. 20% at 1 : 4 compound/lipid ratio) reduction in motional ordering of DMPC side-chains, reflected in the reduction in $\Delta\nu_Q$ and S_{CD}. The assignments are inferred from studies on specifically deuterated phospholipids [14,15].

Proton NMR

Nuclear Overhauser determinations. Fig. 4a shows the proton NMR spectrum of a sonicated codispersion of I and four equivalents of DMPC-d_{54}. Even at 80°C, inclusion of the compound in the membrane slows its

TABLE I

Quadrupolar splittings (in kHz) for multilamellar dispersions at 28°C of DMPC-d_{54} in the absence, and in the presence of increasing molar ratios, of SK&F 96079. Order parameters, S_β (or S_{CD}), are shown in parentheses. Assignments are based on Ref. 14 and Ref. 15.

Deuterium [a] positions	Pure DMPC-d_{54}	Drug/DMPC = 1:20	Drug/DMPC = 1:8	Drug/DMPC = 1:4
2_a 3–6	30.0 (0.239)	29.2 (0.233)	29.2 (0.233)	27.3 (0.218)
8_b, 7_a, 7_b	28.8 (0.230)	28.2 (0.225)	28.4 (0.226)	– [b]
9_b, 8_a	25.8 (0.206)	25.1 (0.200)	23.8 (0.190)	– [b]
10_b, 9_a	24.0 (0.191)	23.4 (0.186)	21.9 (0.175)	21.4 (0.171)
11_b, 10_a, $2_{b'}$	21.2 (0.169)	20.5 (0.163)	18.9 (0.151)	19.7 (0.157)
11_a	20.2 (0.161)	19.6 (0.156)	18.1 (0.144)	16.1 (0.128)
12_b	18.1 (0.144)	17.6 (0.140)	16.2 (0.129)	14.5 (0.116)
12_a	16.2 (0.129)	15.7 (0.125)	14.5 (0.116)	12.7 (0.101)
13_b, 2_b	13.4 (0.107)	13.0 (0.104)	12.0 (0.096)	10.8 (0.086)
13_a	11.6 (0.092)	11.4 (0.091)	11.3 (0.090)	10.8 (0.086)
14	3.8 (0.030)	3.6 (0.029)	3.30 (0.029)	2.8 (0.022)

[a] Numbers denote the individual carbon atoms of the fatty acyl side-chains. The subscripts $_a$ and $_b$ refer to the *sn*-1 and *sn*-2 chains, respectively. The deuterons on the 2 position of the *sn*-2 chain are non-equivalent and are designated 2_b and $2_{b'}$.

[b] Only a single broad peak is observed in the 'plateau' region.

molecular reorientation, resulting in considerable line broadening. A number of signals from the glyceryl and choline moieties of DMPC-d_{54} can be observed, in addition to signals from residual protons in the myristate side-chains. A sonicated dispersion of an equivalent amount of pure I, which is only very sparingly soluble in aqueous medium, in the absence of any DMPC-d_{54}, yields practically no observable signal. Thus, it is reasonable to conclude that the observed signals from the compound in the DMPC-d_{54} codispersion originate from compound incorporated into and solubilised by the membrane environment.

Some typical NOE difference spectra determined on the sonicated codispersion are shown in Figs. 2b to e. Irradiation times varying from between 50 to 500 ms were employed in order to examine NOE buildup rates. Intramolecular NOEs yield some useful information with respect to the membrane bound conformation of I. Apart from the NOEs expected between adjacent protons on the same ring, an NOE builds up rapidly to H5 when the envelope of signals corresponding to the *o*-toluidine ring is irradiated (Fig. 2b), which may be ascribed to proximity between this proton and H6′. The reciprocal NOE (Fig. 2d) is clearly observed. The conformation of I was modelled interactively on an Evans and Sutherland PS-300, allowing free rotation about the N-Cl′ bond. The relatively high field shift of H5 (6.4 ppm) was taken into consideration by ensuring that the final conformations of the toluidine ring relative to the quinoline placed H5 well within the ring-current shielding cone of half-angle 54.7° defined by the axis perpendicular to the plane of the former and passing through its geometric centre. This may be effected interactively by means of software written at SK&F to run on the PS-300. Both the inter-ring NOEs and observed shielding are consistent with the torsion angle defined by C3-C4-N-Cl′ being around −120°, corresponding to an H5-H6′ distance of ca. 3.5 Å.

The NOE experiments on the whole were not very informative regarding the precise location of I in the membrane. Some NOEs, particularly between aromatic signals and signals in the spectral region between ca. 4.0 and 4.8 ppm, could not be reliably assigned to compound-lipid effects because of overlap in the latter region with signals due to the compound, such as arise from its quinoline O-CH_3 group, or the five-membered ring methylenes. Only the signal from the proton on the β-carbon of the glyceryl moiety of DMPC, resonating at low field at ca. 5.2 ppm, can thus be reliably inferred to be involved in NOE's with the included compound (Fig. 2e). Moreover NOEs are seen from the glyceryl β-proton to numerous signals of I, implying considerable mobility of the compound with respect to the head-group region.

The spectrum of II, another (H^+, K^+)-ATPase inhibitor of the same structural class, codispersed and sonicated in the presence of four equivalents of DMPC, is shown in Fig. 3a. This compound is much more water-soluble than I, and yields rather sharp signals, even at 25°C, implying rapid exchange on the ^{1}H-NMR time scale between free and membranous environments. Some typical NOE difference spectra resulting from irradiation of SK&F 96464 protons are shown in Fig. 5b–e. The conformation of II was varied interactively to accommodate the observed NOEs, and the considerable shielding (by ring current effects) of H2 and H3, and deshielding of H5 and H6. Specifically, irradiation of H2, H3 and H5 produces slight NOEs to the envelope of signals at ca. 7.3 ppm corresponding to H7 and the protons directly attached to the *o*-toluidino moiety; irradiation of the H3 resonance also produces an NOE to the 2′-CH_3 signal. A conformation of II defined by

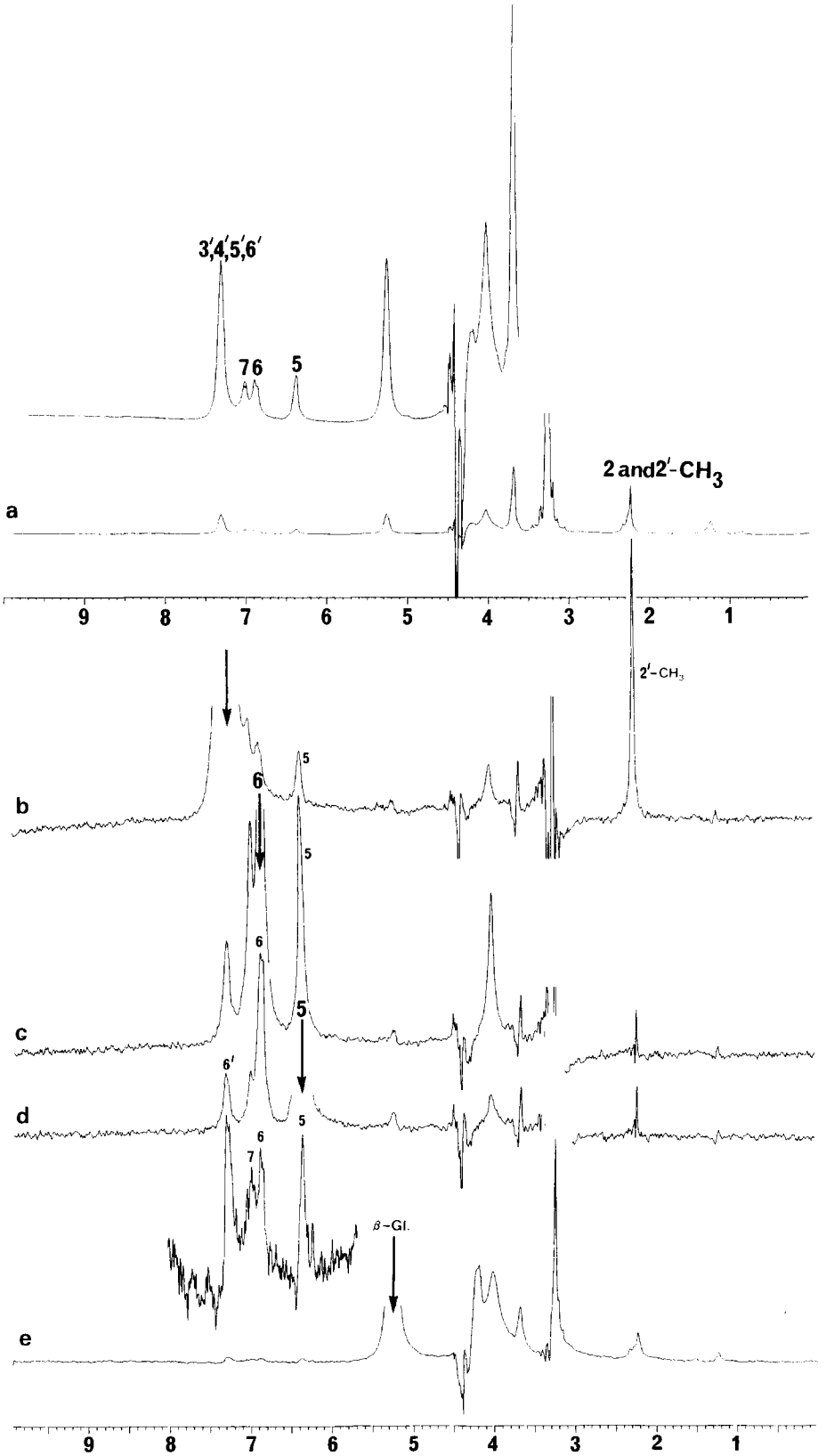

Fig. 2. (a) 360 MHz ^{1}H-NMR spectrum at 80°C of a sonicated aqueous codispersion of 12 mg DMPC-d_{54} and 0.25 mole equivalents of I. Traces (b) to (e) represent NOE difference spectra consequent on irradiation at (b) the *o*-toluidine protons of I (50 ms); (c) the H6 signal of I (50 ms); (d) the H5 signal of I (50 ms); (e) the DMPC glyceryl β-proton (250 ms).

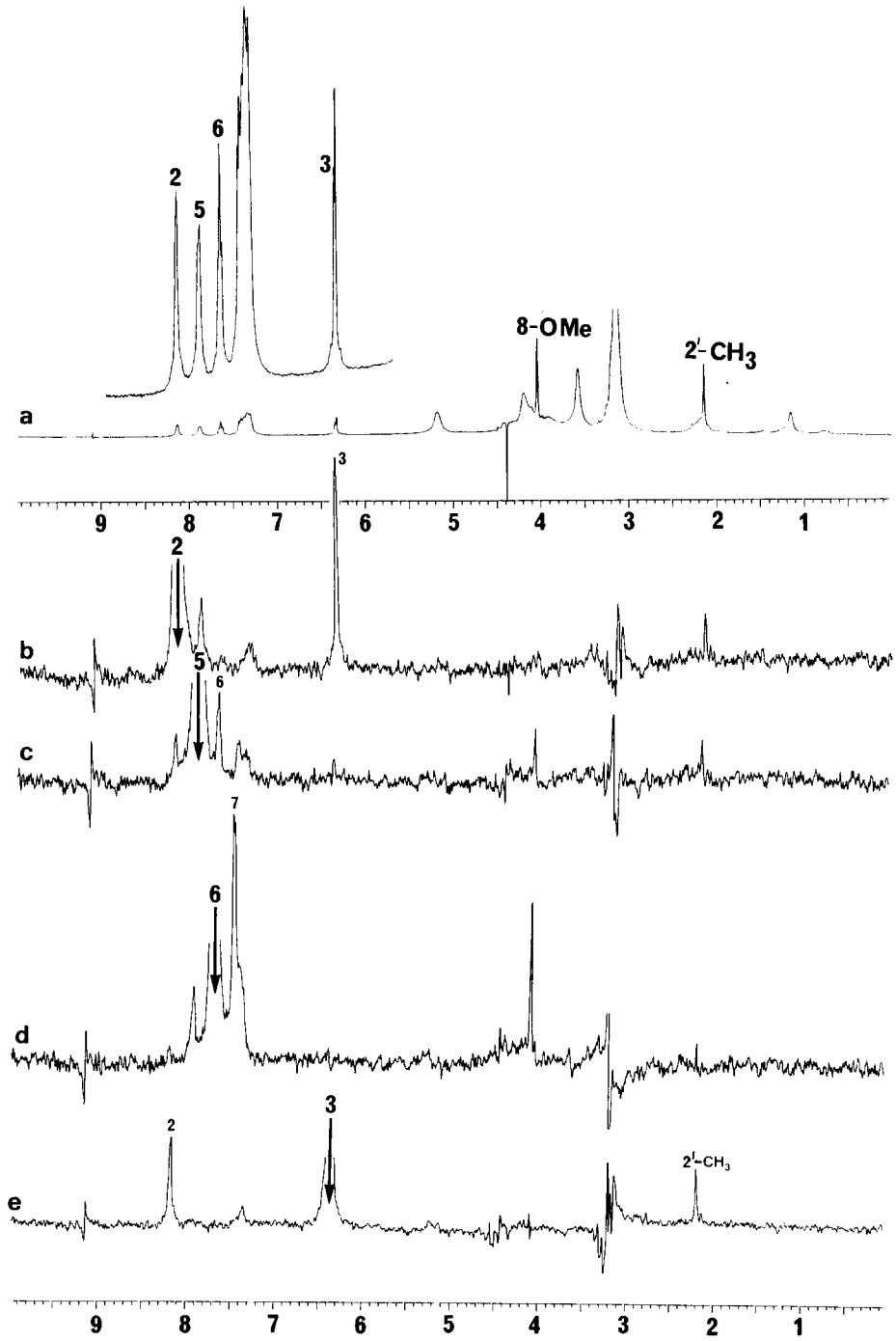

Fig. 3 (a) 360 MHz ^{1}H-NMR spectrum at 25°C of a sonicated aqueous codispersion of 5 mg DMPC-d_{54} and II in a 4:1 molar ratio. (b) to (e) correspond to NOE difference spectra resulting from 250 ms irradiation at the (b) H2 (c) H5 (d) H6 and (e) H3 signals of the compound.

torsion angles of ca. 80° and ca. −105° for the angles defined by C3-C4-N-Cl′ and C4-N-Cl′-C2′ respectively places both H2 and H3 well inside, and H5 and H6 outside the ring current shielding cone centred on the *o*-toluidine. The related conformation produced by a 180° rotation of the *o*-toluidine ring about the Cl′-N bond is also significantly populated. Only very slight NOE's between compound and membrane signals were observed reflecting the significant fraction of the former in the aqueous phase.

Spin probe results. In an attempt to define compound orientation more precisely, spin probe experiments using nitroxide-containing free radicals were performed. Spin-labelled fatty acids have been shown by C-13 relaxation enhancement measurements to partition into model membranes with the paramagnetic centre some-

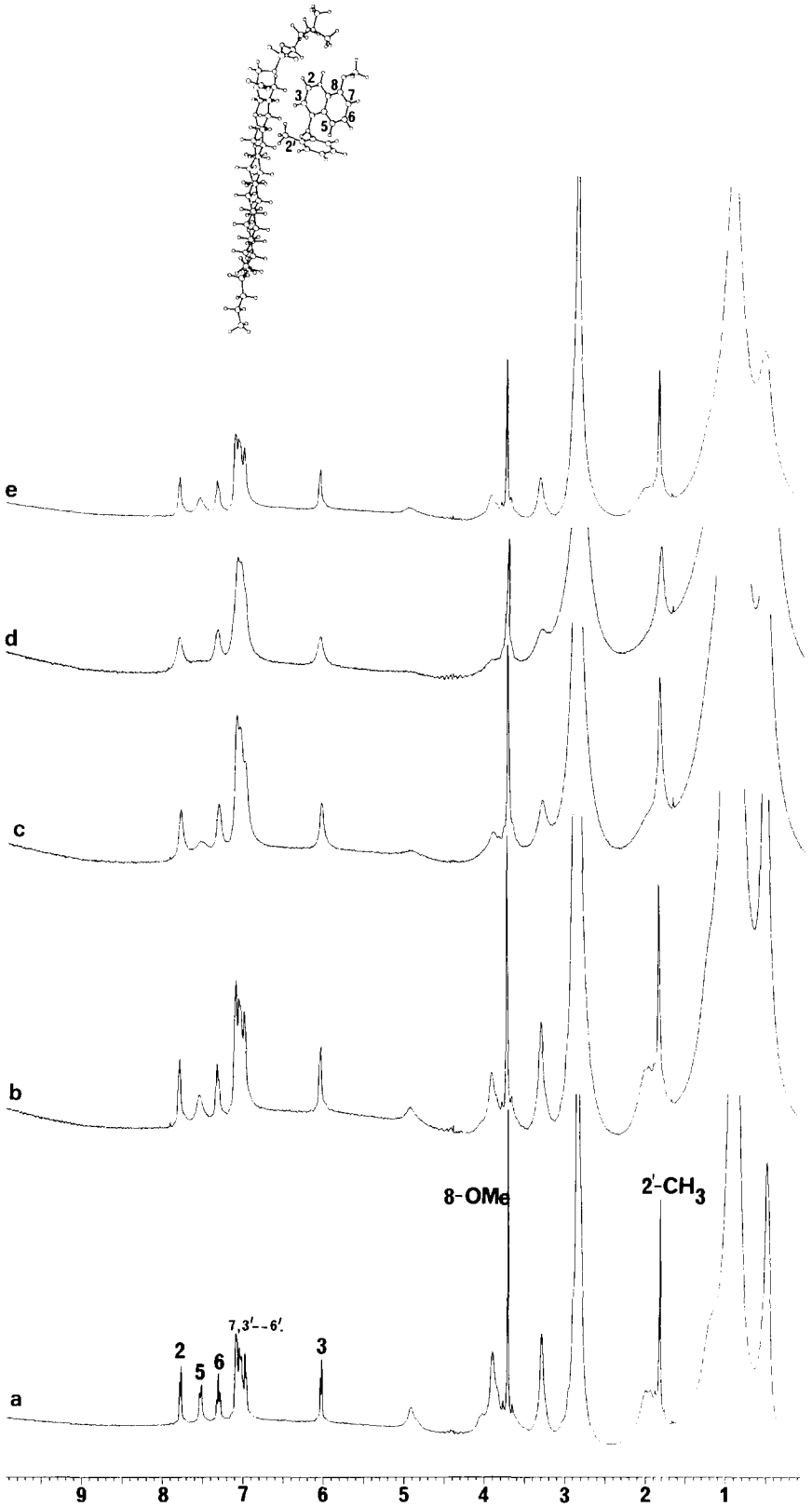

Fig. 4 The effects at 25°C of the incorporation of various amounts of 5-doxyl stearic acid and 16-doxyl stearic acid into a sonicated dispersion of 0.25 mol equivalents of II in DMPC. (a) Control spectrum, corresponding to 0.45 mg II and 5 mg DMPC; (b) after addition of 0.017 mg, (c) 0.050 mg and (d) 0.10 mg 5-doxyl stearic acid; and (e) after addition of 0.10 mg 16-doxyl stearic acid.

what higher than the corresponding side-chain positions [16]. They should thus constitute useful 'depth probes' of the geometry of insertion of compounds into membranes, and have in fact been used to show valinomycin partitioning into the interior of DMPC membranes [17]. Fig. 4 shows the effects of incorporating different mole fractions of 5-doxyl and 16-doxyl stearic acid into sonicated DMPC codispersions with II. Incorporation of the paramagnetic probes into the membrane produces dramatic and differential broadening of signals from both DMPC and compound. The latter effects are much more pronounced with the 5-doxyl than with the 16-

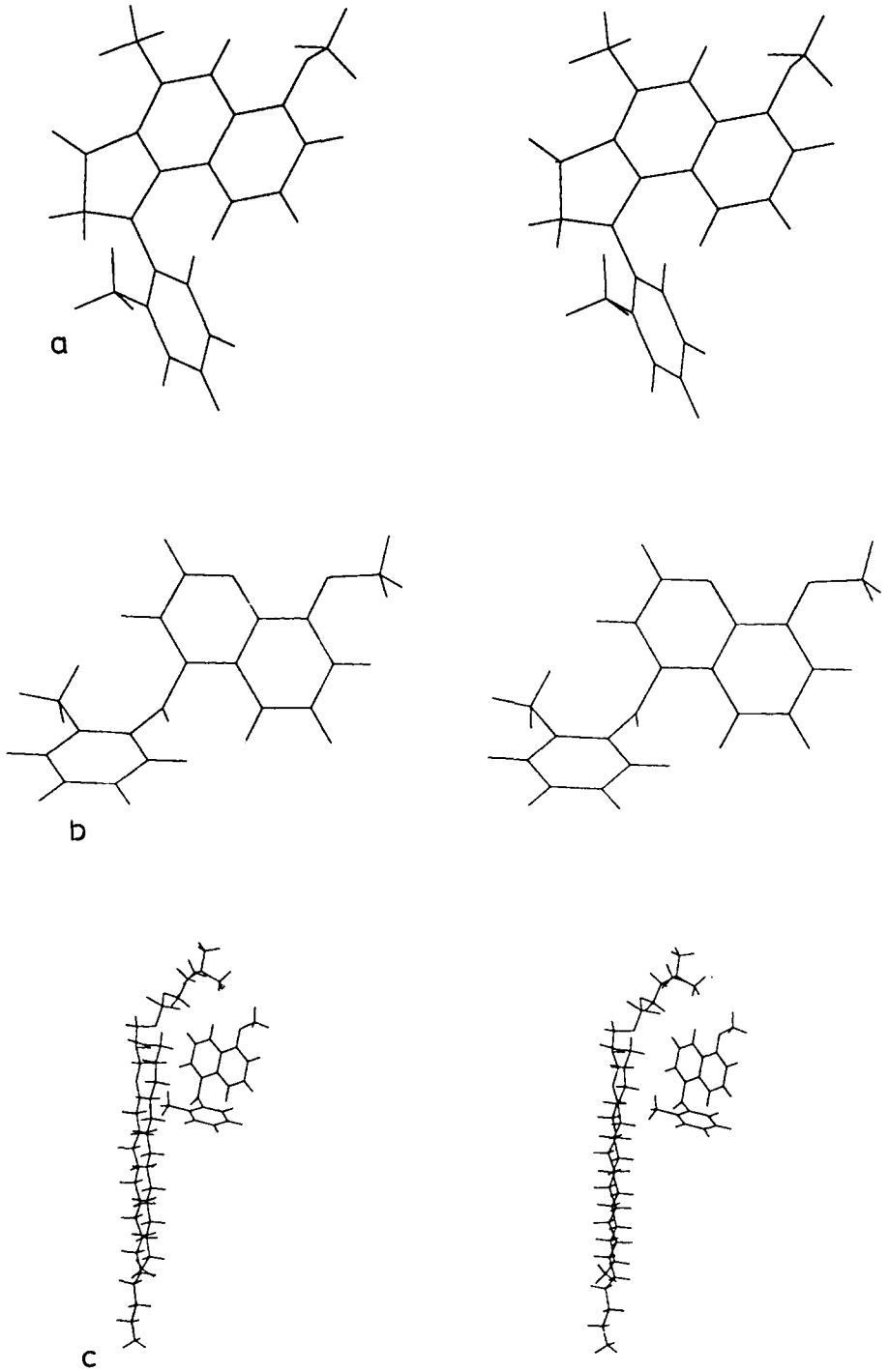

Fig. 5. Stereo plots of membrane bound conformations of (a) I and (b) II, consistent with intermolecular NOEs and ring current perturbations of chemical shifts; (c) a hypothetical complex between a DMPC molecule and II, consistent with fatty acid spin probe data. This structure is only intended to be representative and not unique.

doxyl label, which is consistent with the compound being located at the head-group, and hence much further from the 16- than the 5-substituted probe. The signal from the compound which is most affected is that due to the 5-proton on the quinoline ring, followed by that from the 2-methyl group of the ortho-toluidine moiety. The signals from the other ring protons broaden much more slowly with increasing amounts of probe lipid, with that from the quinoline 8-position *O*-methyl group remaining sharpest.

In a control experiment, II was co-dispersed and sonicated with 5-doxyl stearic acid in the absence of DMPC. Although an identical amount broaden the signal from the quinoline 5-proton of II beyond detection, no effect was seen in the absence of DMPC. It may thus be concluded that the differential broadening caused by the probe in the membranous system reflects a specific location and limited family of orientations and conformations of II.

Analogous experiments with I produced dramatic but much less specific broadening (results not shown). This is ascribed to this compound adopting a number of different orientations in the bilayer, rapid exchange between which would serve to average out the broadening effects of the fatty acid probe. The possible origins of these differences between the two compounds are discussed in the next section.

Discussion

Fig. 5a and b shows stereo plots of the NOE derived conformations of I and II respectively, consistent with intramolecular NOEs and ring-current shielding and deshielding influences.

At the roughly physiological pH values of this study, the dissociation constants of the compounds suggests that both I ($pK_a = 9.54$) and II ($pK_a = 8.63$) will be largely cationic due to protonation on the quinoline nitrogen (Mitchell, R.C., unpublished data). Under these circumstances II can make two favourable electrostatic interactions with the DMPC head-group, which were modelled using the head-group conformations for DMPC derived by Seelig et al. [18]. Hydrogen bonds can be found between the amino NH proton of the compound and the *sn*-1 side-chain carbonyl of a DMPC molecule, and between the NH group of the protonated quinoline ring of the compound and a primary phosphodiester oxygen of the same DMPC molecule. The resultant orientation, shown in Fig. 5c, positions the quinoline 5-proton deepest in the bilayer, and the $-OCH_3$ group shallowest, consistent with the fatty acid spin probe results. Also consistent with these results is the appreciable depth of the ortho-toluidine methyl group in the bilayer.

This interaction scheme would also serve to explain the NOE's observed between the compound and the glyceryl β-proton of DMPC. It is unrealistic to propose such a well-defined membrane orientation for I, given the non-specific nature of the intermolecular NOE and spin probe data. Both sets of results, however, are consistent with the compounds partitioning into the head-group region. It is significant that the amino NH proton which stabilises a specific orientation of II, is lacking in I. It would appear that at least two geometrically favourable electrostatic contacts are necessary to confer orientational specificity on the compound.

The FT-IR, DSC and ^{2}H-NMR results show that although I is highly lipophilic it does not have any gross effects on phospholipld bilayer structure, the main effect being a reduction in the co-operativity of the gel to liquid crystalline phase transition. Compounds of this structural class would thus not be predicted to display the deleterious toxic properties, principally haemolytic, which was observed in previous studies of the amphiphilic SK&F 95018 (III). This compound, a promising mixed β-blocker and vasodilator, profoundly disrupts model bilayers to non-ordered, probably micellar systems [19].

References

1 Ganser, A.L. and Forte, J.G. (1973) Biochim. Biophys. Acta 307, 169–180.
2 Sachs, G., Chang, K.H., Rabon, E., Schackmann, R., Lewin, M. and Saccomani, G. (1974) J. Biol. Chem. 251, 7690–7698.
3 Smolka, A., Helander, H.F. and Sachs, G. (1983) Amer. J. Physiol. 245, G589–96.
4 Di Bona, D.R., Ito, S., Berglindh, T. and Sachs, G. (1979) Proc. Natl. Acad. Sci. USA 76, 6689–6693.
5 Black, J.W., Duncan, W.A.M., Durant, G.J., Ganellin, C.R. and Parsons, E.M. (1972) Nature 236, 385–390.
6 Sachs, G., Carlsson, E., Lindberg, P. and Wallmark, B. (1988) Ann. Rev. Pharmacol. Toxicol. 28, 269–84.
7 Beil, W., Hackbarth, I. and Sewing, K.-Fr. (1986) Br. J. Pharmacol. 88, 19–23.
8 Scott, C.K., Sundell, E. and Castrovilly, L. (1987) Biochem. Pharmacol. 36, 97–104.
9 Wallmark, B., Briving, C., Fryklund, J., Munson, K., Jackson, R., Mendlein, J., Rabon, E. and Sachs, G. (1987) J. Biol. Chem. 262, 2077–2084.
10 Ariens, E.J. (1987) Medicinal Res. Rev. 7, 367–387.
11 Ariens E.J. and Simonis, A.M. (1960) Arch. Int. Pharmacodyn. 1960, 479–496.
12 Casal, H.L. and Mantsch, H.H. (1984) Biochim. Biophys. Acta 779, 381–401.
13 Haasnoot, C.A.G. (1983) J. Magn. Reson. 52, 153–158.
14 Seelig, J. (1977) Q. Rev. Biophys. 10, 353–418.
15 Davis, J.H. (1979) Biophys. J. 27, 339–358.
16 Ellena, J.F., Archer, S.J., Dominey, R.N., Hill, B.D. and Cafiso, D.S. (1988) Biochim. Biophys. Acta 940, 63–70.
17 Meers, P. and Feigenson, G.W. (1988) Biochim. Biophys. Acta 938, 469–482.
18 Seelig, J., Gally, H.U. and Wohlgemuth, R. (1977) Biochim. Biophys. Acta 467, 109–119.
19 Jones, H.B., Reid, D.G. and Luke, J.S. (1989) Toxicol. In Vitro 3, 299–309.